Atypical inferoseptal accessory pathway connection associated with an aneurysm of the coronary sinus: Insight from a three-dimensional combined image of electroanatomic…

Nishimori, Makoto ; Kiuchi, Kunihiko ; Mori, Shumpei ; Kurose, Jun ; Izawa, Yu ; Kouno, Shingo ; Nakagawa, Hiroaki ; Shimoyama, Shinsuke ;…

(Citation)
HeartRhythm Case Reports,4(9):389-392

(Issue Date)
2018-09

(Resource Type)
journal article

(Version)
Version of Record

Atypical inferoseptal accessory pathway connection associated with an aneurysm of the coronary sinus: Insight from a three-dimensional combined image of electroanatomic mapping and computed tomography

Makoto Nishimori, MD,* Kunihiko Kiuchi, MD, FHRS,* Shumpei Mori, MD, PhD,* Jun Kurose, MD,* Yu Izawa, MD,* Shingo Kouno, MD,* Hiroaki Nakagawa, MD,* Shinsuke Shimoyama, MD,† Koji Fukuzawa, MD, PhD,* Ken-ichi Hirata, MD, PhD*

*From the *Division of Cardiovascular Medicine, Department of Internal Medicine, Kobe University Graduate School of Medicine, Kobe, Japan, and †Department of Radiology, Kobe University Graduate School of Medicine, Kobe, Japan.*

Introduction

Inferoseptal accessory pathways are associated in some cases with a coronary sinus (CS) aneurysm or diverticulum.[1,2] A single aneurysm of the CS or its tributaries has been detected in 9% of patients treated for inferoseptal accessory pathways.[3,4] Whereas ablation of accessory atrioventricular (AV) pathways has a high success rate, ablation of inferoseptal accessory pathways is difficult compared to ablation at other locations.[5,6] Electrophysiologists need detailed anatomic knowledge of the inferoseptal space, and hopefully computed tomographic (CT) integration into electroanatomic mapping would be useful in determining the anatomy to allow successful ablation. To the best of our knowledge, this is the first case of an accessory pathway associated with a CS aneurysm that was precisely ablated using a three-dimensional (3D) combined image of electroanatomic mapping and CT.

KEY TEACHING POINTS

- Inferior accessory pathways are occasionally associated with a coronary sinus (CS) aneurysm. A district accessory pathway potential can be recorded at the neck of the CS aneurysm.
- The neck of the CS aneurysm was in direct contact with the mitral annulus. The accessory pathway was long and connected the left atrium and right ventricle epicardially with an oblique course.
- Combining the computed tomography image and electroanatomic mapping can be useful in patients with a complicated abnormal anatomy.

Case report

A 45-year-old woman who experienced palpitations for 2 hours and suffered from a cardiac pulmonary arrest was admitted to the emergency room. An electrocardiogram (ECG) showed ventricular fibrillation, which terminated after the third electrical defibrillation. The surface ECG in sinus rhythm exhibited preexcitation with negative delta waves in leads III, aVF, aVR, and V_1, positive delta waves in leads I, aVL, and V_2 to V_6, and isoelectric delta waves in lead II (Figure 1A), suggesting the presence of a right inferoseptal accessory pathway.

Contrast-enhanced cardiac magnetic resonance imaging revealed normal cardiac function without any late gadolinium enhancement but contingently revealed an aneurysm of the CS. Although at first Wolff-Parkinson-White syndrome was considered to be the cause of the ventricular fibrillation, a subcutaneous implantable cardiac defibrillator eventually was implanted as secondary prevention for sudden cardiac death because there was no evidence of an etiology. Three-dimensional CT was performed, focusing on the tricuspid and mitral annuli and inferior pyramidal space where the CS aneurysm was located. Epicardial adipose tissue surrounding both AV junctions was reconstructed along with the CS and CS aneurysm (Figure 2). The CS itself was located on the left atrial side of the left AV junction. A large sessile CS aneurysm (26 mm × 31 mm) originated from the

KEYWORDS Computed tomography; Coronary sinus aneurysm; Inferior accessory pathway; Inferior pyramidal space; Radiofrequency catheter ablation; Three-dimensional combined image
(Heart Rhythm Case Reports 2018;4:389–392)

Address reprint requests and correspondence: Dr Kunihiko Kiuchi, Division of Cardiovascular Medicine, Department of Internal Medicine, Kobe University Graduate School of Medicine, Kunihiko Kiuchi, 7-5-2, Kusunoki-cho, Chuo-Ku, Kobe, 650-0017, Japan. E-mail address: kunihikokiuchi@yahoo.co.jp.

https://doi.org/10.1016/j.hrcr.2018.04.009

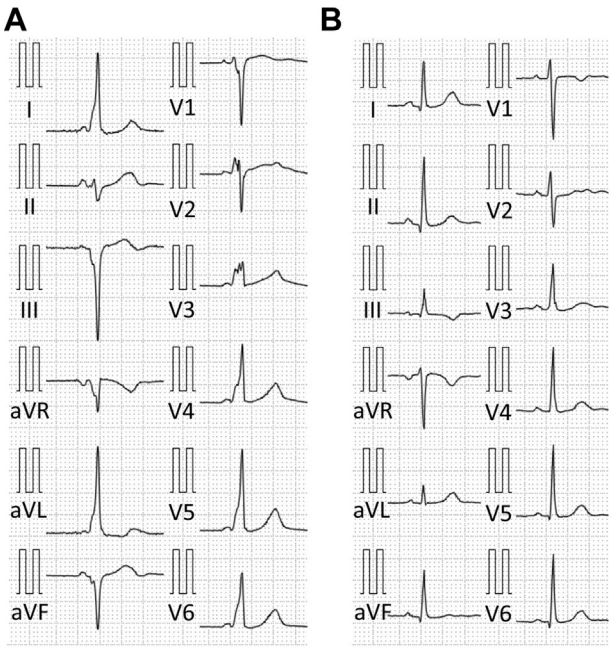

Figure 1 Twelve-lead surface electrocardiogram recorded during sinus rhythm before (**A**) and after (**B**) ablation.

bifurcation of the inferior interventricular vein and was located just beneath the basal inferior left ventricle in contact with the mitral valve annulus at its neck. However, the tricuspid valve annulus was insulated from the CS aneurysm by intervening adipose tissue within the inferior pyramidal space (Figure 2). Fluoroscopy-like images were reconstructed to guide the subsequent radiofrequency catheter ablation procedure (Figure 2).

Conventional multipolar catheters were introduced into the right atrium, right ventricle, and CS, and CS venography was performed. An electrophysiological study demonstrated that the accessory pathway anterograde effective refractory period and block rate were 310 ms and 200 ppm, respectively. Although orthodromic AV reentrant tachycardia was reproducibly induced by extrastimulation, atrial fibrillation could not be induced. Therefore, the shortest R-R interval of the accessory pathway during atrial fibrillation could not be measured. A detailed activation map of the CS and aneurysm was performed using the EnSite NavX system (St. Jude Medical, St. Paul, MN) integrated with 3D CT. To create the integrated fusion image, the CS catheter was used to align the CS reconstructed by CT (Figure 3A–C). The earliest retrograde atrial activation was recorded on the inferoseptal left atrial wall on the mitral annulus at the neck of the CS aneurysm (Figure 3A and B). The earliest anterograde ventricular activation was recorded deep inside the aneurysm and then propagated onto the inferoseptal wall on the tricuspid annulus (Figure 3C). An accessory pathway potential could be recorded from the neck of the aneurysm where the earliest retrograde atrial activation could be recorded (Figure 3C). A single radiofrequency application with an irrigated ablation catheter (TactiCath, Abbott, St. Paul, MN) at the neck of the CS aneurysm could eliminate both the anterograde and retrograde conduction (Figure 3D–H). The preexcitation on the surface ECG disappeared (Figure 1B).

Discussion

Accessory pathways in the CS are reportedly associated with abnormal embryologic development of the sinus venous and remnant of the muscle sheath that surrounds the proximal CS.[7] To the best of our knowledge, this is the first report to reveal the electrical and anatomic features of an atypical inferoseptal accessory pathway associated with a CS

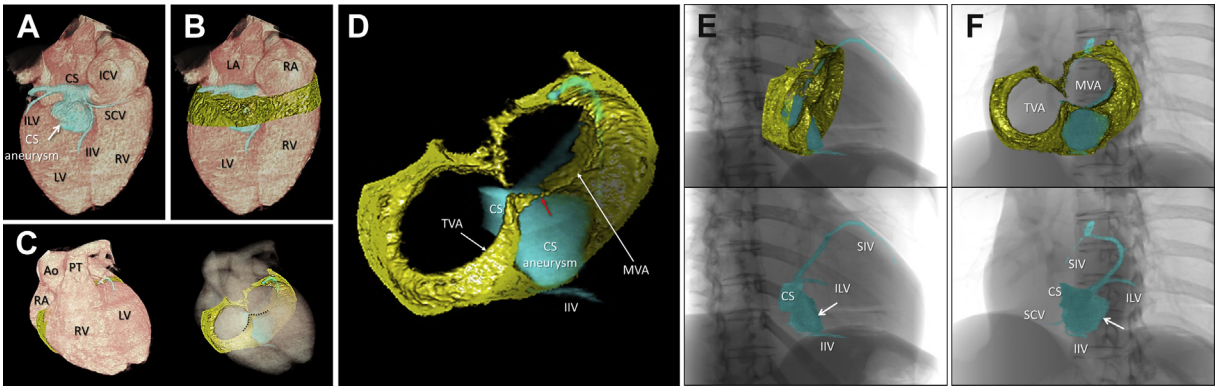

Figure 2 **A:** Volume-rendered image reconstructed using cardiac computed tomography showing the location of the coronary sinus. **B–D:** Images of the epicardial adipose tissue surrounding both atrioventricular (AV) junctions and the inferior pyramidal space (*black-dotted line*) were reconstructed. When viewed from the anterosuperior direction, the transparency of the cardiac volume was increased (**C**) and the volume data of the AV epicardial adipose tissue along with the coronary venous system could be obtained (**D**), which were integrated with the electroanatomic mapping (see Figure 3). The coronary sinus (CS) was located on the left atrial side of the left AV junction (**A**). The CS aneurysm originated from the bifurcation of the inferior interventricular vein (IIV) and small cardiac vein (SCV), and was located just beneath the basal inferior left ventricle in contact with mitral valve annulus (MVA) at its neck (**D**). *Red arrow* in D indicates the estimated site of the accessory pathway. **E, F:** Fluoroscopy-like volume-rendered images were reconstructed to guide the procedure using cardiac computed tomography, as shown from the 30° right anterior oblique (**E**) and 45° left anterior oblique (**F**) views. Note the consistency of the fluoroscopic images during the procedure (see Figure 3). *White arrows* indicate the CS aneurysm. Ao = ascending aorta; ICV = inferior caval vein; ILV = inferolateral vein; LA = left atrium; LV = left ventricle; PT = pulmonary trunk; RA = right atrium; RV = right ventricle; SIV = superior interventricular vein; TVA = tricuspid valve annulus.

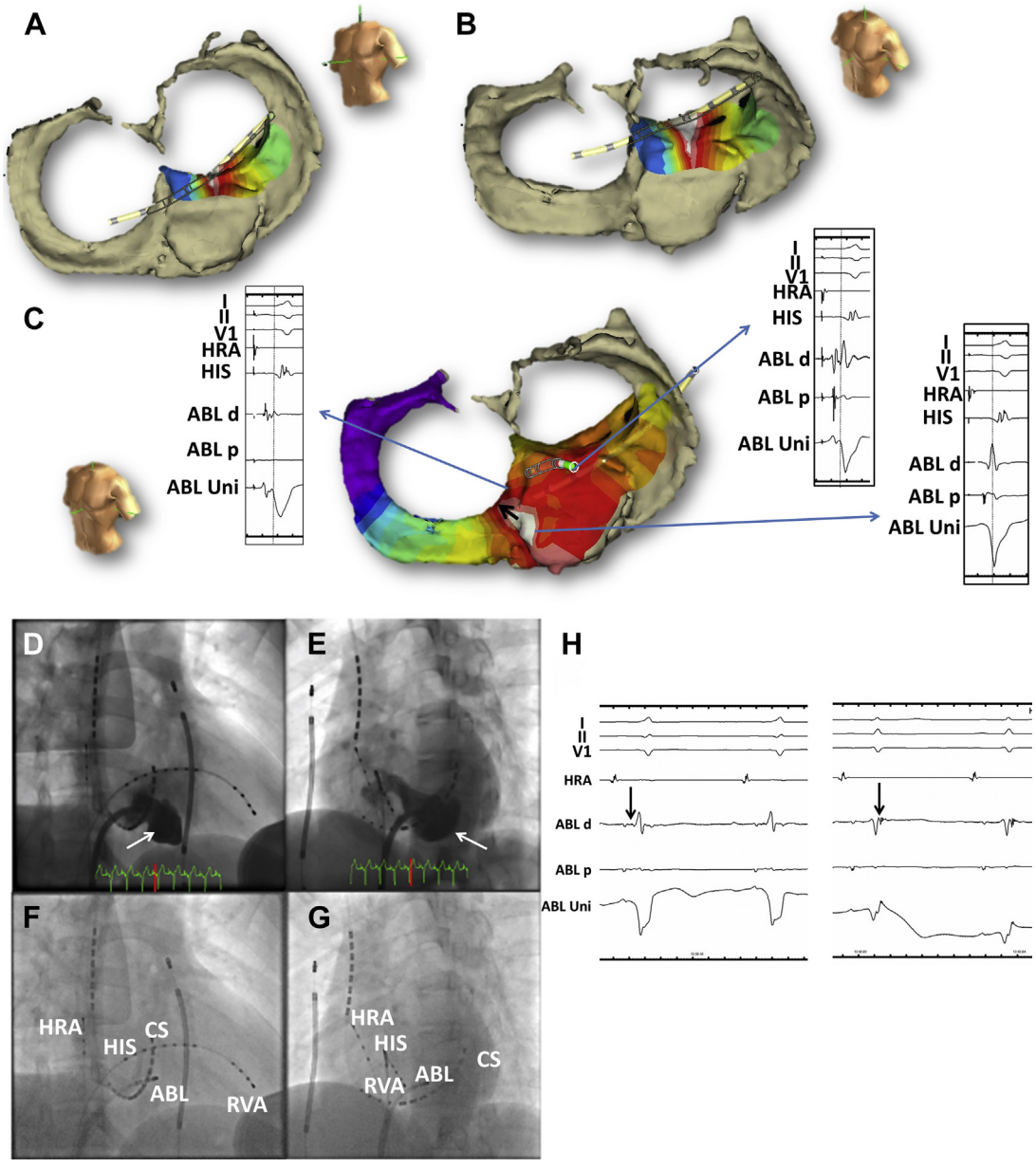

Figure 3 **A, B:** Earliest atrial activation site assessed by the NavX system integrated with three-dimensional (3D) computed tomography (CT) in the left anterior oblique (**A**) and slightly cranial (**B**) views. **C:** Earliest ventricular activation site assessed by the NavX system integrated with 3D CT. Whereas a distinctive accessory pathway potential could be recorded at the neck of the coronary sinus (CS) aneurysm, the local ventricular activation was earlier deep within the aneurysm, where the unipolar electrogram confirmed a continuous P-QS morphology. The earliest ventricular activation likely spread toward the right inferoseptal wall near the tricuspid annulus but not the left ventricle (*black arrow*). The right and left panels show the local electrograms and surface electrocardiogram. The *dotted line* indicates the onset of the delta wave. **D, E:** CS venograms shown from the right anterior oblique (RAO) 30° (**D**) and left anterior oblique (LAO) 45° (**E**) views. *White arrows* indicate the CS aneurysm. **F, G:** Successful ablation catheter position shown in the RAO 30° (**F**) and LAO 45° (**G**) views. Of note, the successful ablation site was at the neck of the CS aneurysm, where a distinctive accessory pathway potential could be recorded. **H:** After the accessory pathway was eliminated, a sharp accessory pathway potential was documented after the ventricular potential (*black arrows*). This indicated that the accessory pathway could be eliminated at a more proximal site before it spread extensively toward the right ventricle. ABL = ablation catheter; HIS = His bundle; HRA = high right atrium; RVA = right ventricular apex.

aneurysm by using a NavX system integrated with the true anatomy obtained by CT reconstruction.

In the current case, from the surface ECG we estimated that the accessory pathway was located on the right inferoseptal wall, according to the conventional algorithm.[8] Unfortunately, no ECG features, including a steep positive delta wave on lead aVR and deep S wave on lead V_6 suggesting an epicardial accessory pathway, subsequently could be documented.[9] This suggested that a right inferoseptal accessory pathway could not be associated with the CS aneurysm. However, the earliest retrograde activation was recorded at the left inferoseptal wall. To assess the ECG discrepancy, a detailed anatomic assessment, focusing on the inferior pyramidal space[10–12] around the CS aneurysm, was performed

using 3D CT. The activation map fused with 3D CT could clearly demonstrate that this atypical accessory pathway was a long one with an oblique course along the CS aneurysm. The atrial insertion site was located at the left inferoseptal wall, whereas the ventricular insertion site was located on the right inferoseptal wall, which could explain why the polarity of the delta waves on the surface ECG indicated a right inferoseptal origin. On the surface ECG, the distinction between a right or left inferoseptal accessory pathway should be made based on the presumed site of the ventricular insertion.[13]

In this case, an accessory pathway potential could be recorded at the neck of the CS aneurysm, which was common and consistent with previous reports.[6,14] However, few reports have clarified the accurate anatomic relationship between the CS aneurysm and AV junction. In the present case, the neck of the CS aneurysm was in direct contact with the mitral annulus but not the tricuspid annulus. We could speculate that the accessory pathway is located near this point based on this anatomic information. Actually, the atrial insertion site as well as an accessory pathway potential were recorded in that region (Figure 3A–C), where a single radiofrequency application could eliminate the accessory pathway. A preprocedural anatomic evaluation would provide the clue to allow a smart and safe ablation in this case.

As shown in Figure 3A–C, we created for the first time a fusion image made using electroanatomic mapping and the volume data of the epicardial adipose tissue obtained from CT. Usually, electroanatomic mapping is integrated with the volume data of the cardiac chamber of interest, which is enhanced by contrast material. Although the feasibility and utility of this fusion technique needs further investigation, its integration with the volume-rendered substance of the nonenhanced tissue, including the epicardial fat and/or myocardium, would be an attractive option to correctly reflect the epicardial and/or myocardial structural anatomy into the ablation procedure. As a matter of course, the target for ablation would not be a chamber but always a wall or partition constructing the structure. Of interest, a previous study reported the difficulty of achieving successful ablation in patients with a CS aneurysm even using a conventional 3D mapping system.[15]

Conclusion

We present the case of an atypical inferoseptal accessory pathway associated with a CS aneurysm. The 3D CT could visualize the close proximity of the inferoseptal mitral annulus to the neck of the CS aneurysm, where a distinctive accessory pathway potential could be recorded. Preprocedural detailed anatomic assessment using 3D CT would be useful in determining the potential location of the accessory pathway associated with a CS aneurysm and facilitating a simple and smooth ablation procedure without increasing the risk of complications.

Acknowledgments

The authors would like to thank Mr John Martin for his linguistic assistance.

References

1. Boulos M, Gepstein L. Electroanatomical mapping and radiofrequency ablation of an accessory pathway associated with a large aneurysm of the coronary sinus. Europace 2004;6:608–612.
2. Al Fagih A, Al Zahrani G, Al Hebaishi Y, Dagriri K, Al Ghamdi SA. Coronary sinus diverticulum as a cause of resistant posteroseptal pathway ablation. J Saudi Heart Assoc 2011;23:41–44.
3. Guiraudon GM, Guiraudon CM, Klein GJ, Sharma AD, Yee R. The coronary sinus diverticulum: a pathologic entity associated with the Wolff-Parkinson-White syndrome. Am J Cardiol 1988;62:733–735.
4. Weiss C, Cappato R, Willems S, Meinertz T, Kuck KH. Prospective evaluation of the coronary sinus anatomy in patients undergoing electrophysiologic study. Clin Cardiol 1999;22:537–543.
5. Tebbenjohanns J, Pfeiffer D, Jung W, Manz M, Lüderitz B. Radiofrequency catheter ablation of a posteroseptal accessory pathway within a coronary sinus diverticulum. Am Heart J 1993;126:1216–1219.
6. Payami B, Shafiee A, Shahrzad M, Kazemisaeed A, Davoodi G, Yaminisharif A. Posteroseptal accessory pathway in association with coronary sinus diverticulum: electrocardiographic description and result of catheter ablation. J Interv Card Electrophysiol 2013;38:43–49.
7. Sun Y, Arruda M, Otomo K, Beckman K, Nakagawa H, Calame J, Po S, Spector P, Lustgarten D, Herring L, Lazzara R, Jackman W. Coronary sinus-ventricular accessory connections producing posteroseptal and left posterior accessory pathways: incidence and electrophysiological identification. Circulation 2002;106:1362–1367.
8. Chiang CE, Chen SA, Teo WS, et al. An accurate stepwise electrocardiographic algorithm for localization of accessory pathways in patients with Wolff-Parkinson-White syndrome from a comprehensive analysis of delta waves and R/S ratio during sinus rhythm. Am J Cardiol 1995;76:40–46.
9. Takahashi A, Shah DC, Jais P, Hocini M, Clementy J, Haissaguerre M. Specific electrocardiographic features of manifest coronary vein posteroseptal accessory pathways. J Cardiovasc Electrophysiol 1998;9:1015–1025.
10. Mori S, Fukuzawa K, Takaya T, Takamine S, Ito T, Fujiwara S, Nishii T, Kono AK, Yoshida A, Hirata K. Clinical structural anatomy of the inferior pyramidal space reconstructed within the cardiac contour using multidetector-row computed tomography. J Cardiovasc Electrophysiol 2015;26:705–712.
11. Mori S, Nishii T, Takaya T, Kashio K, Kasamatsu A, Takamine S, Ito T, Fujiwara S, Kono AK, Hirata K. Clinical structural anatomy of the inferior pyramidal space reconstructed from the living heart: three-dimensional visualization using multidetector-row computed tomography. Clin Anat 2015;28:878–887.
12. Ichibori H, Mori S, Takaya T, Kiuchi K, Ito T, Fujiwara S, Fukuzawa K, Tatsumi K, Tanaka H, Nishii T, Kono AK, Hirata K. Slit-like deformation of the coronary sinus orifice due to compression of the inferior pyramidal space by the severely dilated left ventricle. Pacing Clin Electrophysiol 2016;39:1026–1029.
13. Huang SKS, Wood MA, eds. Catheter Ablation of Cardiac Arrhythmias. Philadelphia, PA: Saunders/Elsevier; 2006:402.
14. Selvaraj RJ, Sarin K, Singh VR, Satheesh S, Pillai AA, Kumar M, Balachander J. Radiofrequency ablation of posteroseptal accessory pathways associated with coronary sinus diverticula. J Interv Card Electrophysiol 2016;47:253–259.
15. Kerst G, Weig HJ, Weretka S, Seizer P, Hofbeck M, Gawaz M, Schreieck J. Contact force-controlled zero-fluoroscopy catheter ablation of right-sided and left atrial arrhythmia substrates. Heart Rhythm 2012;9:709–714.